Vol. 50, No. 8

Model for Intracellular Lamivudine Metabolism in Peripheral Blood Mononuclear Cells Ex Vivo and in Human Immunodeficiency Virus Type 1-Infected Adolescents

Zexun Zhou,[1] John H. Rodman,[2] Patricia M. Flynn,[3] Brian L. Robbins,[2,3]
Carrie K. Wilcox,[2] and David Z. D'Argenio[1]*

Department of Biomedical Engineering, University of Southern California, Los Angeles, California 90089[1]; Department of Pharmaceutical Sciences, St. Jude Children's Research Hospital, Memphis, Tennessee 38105[2]; and Department of Infectious Diseases, St. Jude Children's Research Hospital, Memphis, Tennessee 38105[3]

The pharmacologic variability of nucleoside reverse transcriptase inhibitors such as lamivudine (3TC) includes not only systemic pharmacokinetic variability but also interindividual differences in cellular transport and metabolism. A modeling strategy linking laboratory studies of intracellular 3TC disposition with clinical studies in adolescent patients is described. Data from ex vivo laboratory experiments using peripheral blood mononuclear cells (PBMCs) from uninfected human subjects were first used to determine a model and population parameter estimates for 3TC cellular metabolism. Clinical study data from human immunodeficiency virus type 1-infected adolescents were then used in a Bayesian population analysis, together with the prior information from the ex vivo analysis, to develop a population model for 3TC systemic kinetics and cellular kinetics in PBMCs from patients during chronic therapy. The laboratory results demonstrate that the phosphorylation of 3TC is saturable under clinically relevant concentrations, that there is a rapid equilibrium between 3TC monophosphate and diphosphate and between 3TC diphosphate and triphosphate, and that 3TC triphosphate is recycled to 3TC monophosphate through a 3TC metabolite that remains to be definitively characterized. The resulting population model shows substantial interindividual variability in the cellular kinetics of 3TC with population coefficients of variation for model parameters ranging from 47 to 87%. This two-step ex vivo/clinical modeling approach using Bayesian population modeling of 3TC that links laboratory and clinical data has potential application for other drugs whose intracellular pharmacology is a major determinant of activity and/or toxicity.

Highly potent combination antiretroviral therapy has significantly reduced the mortality and morbidity of individuals infected with human immunodeficiency virus type 1 (HIV-1) (14, 29). Because of pharmacologic, virologic, immunologic, and behavioral differences among individuals, however, not all patients receive the optimal therapeutic benefit from antiretroviral therapy (8). Initial therapy for HIV-1-infected patients usually consists of two nucleoside/nucleotide reverse transcriptase inhibitors (NRTIs) (e.g., zidovudine [ZDV] and lamivudine [3TC]) and either a nonnucleoside reverse transcriptase inhibitor or a protease inhibitor (5). Although initial therapy is effective for a high proportion of patients, treatment failure and toxicity remain substantial problems, and pharmacokinetic variability can be an important contributing factor. Studies have shown that individualized therapy that controls for the systemic pharmacokinetic variability of indinavir, ZDV, and 3TC can improve the virological outcome relative to that of conventional fixed-dose therapy (9).

For NRTIs like ZDV and 3TC, pharmacologic variability includes not only systemic pharmacokinetic variability but also interindividual differences in cellular transport and metabolism. All NRTIs must cross the cell membrane and undergo stepwise phosphorylation by intracellular kinases to their active triphosphate forms (10, 13). The active triphosphate then inhibits viral replication through competitive binding to the viral enzyme reverse transcriptase and chain reaction termination after incorporation into the proviral DNA (13). The triphosphate anabolite is also a source of toxicity through the inhibition of mitochondrial DNA polymerase (1, 16, 24). While some previous studies have examined intracellular ZDV and 3TC triphosphates (1, 34), and others have previously explored the associations between intracellular triphosphates and anti-HIV activity (34), quantitative models for the intracellular metabolism of NRTIs are lacking.

The hypothesis underlying this report is that the cellular pathways that govern the rate and extent of formation of lamivudine triphosphate are primary determinants of antiviral activity and toxicity of 3TC, similar to other nucleoside analogs that require phosphorylation in target cells. While extracellular concentration and variability in systemic pharmacokinetics will affect the delivery of parent 3TC to target cells in patients, intracellular transport and phosphorylation will be major factors influencing the persistence of 3TC triphosphate. Laboratory studies of intracellular 3TC kinetics can examine intracellular determinants of active 3TC triphosphate kinetics, but they are not necessarily reflective of its disposition in lymphocytes of HIV-1-infected patients. Clinical studies, in contrast, are limited by the intracellular 3TC metabolite data that can be obtained from HIV-1-infected patients. This report presents a

* Corresponding author. Mailing address: Department of Biomedical Engineering, University of Southern California, 1042 Downey Way, DRB 140, Los Angeles, CA 90089. Phone: (213) 740-0341. Fax: (213) 740-0343. E-mail: dargenio@bmsr.usc.edu.
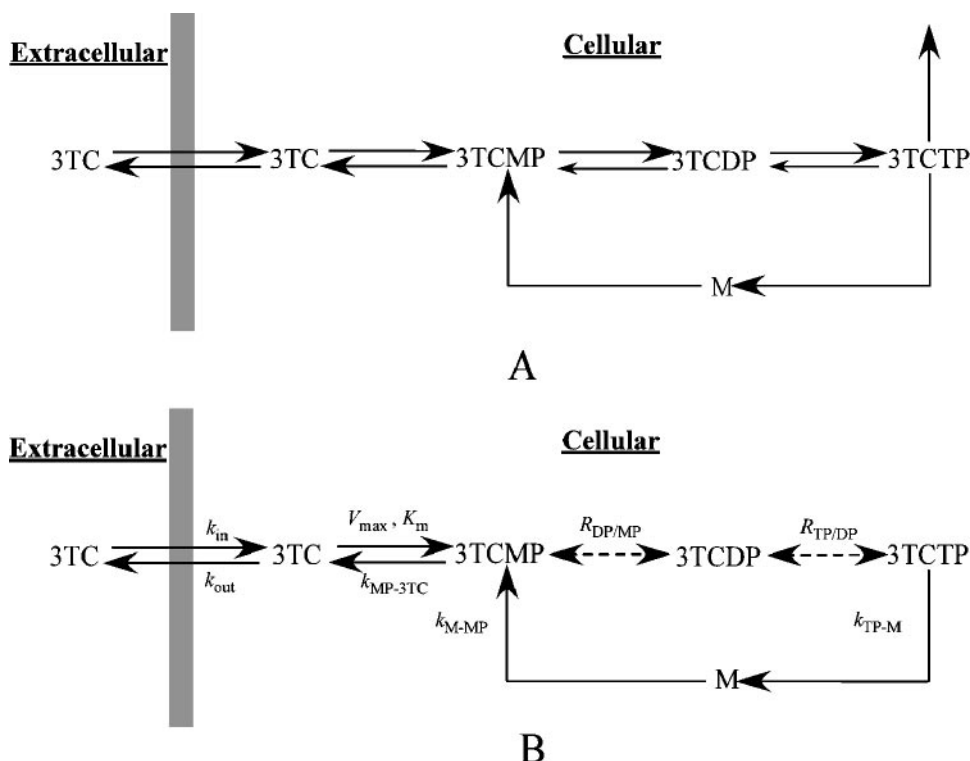
FIG. 1. (A) Pathway model of 3TC transport and metabolism in PBMCs denoting 3TC uptake and efflux and the formation and degradation by phosphatases for 3TCMP, 3TCDP, and 3TCTP. (B) Final model for transport and intracellular metabolism of 3TC obtained from the population analysis of the ex vivo data. See the text for the rationale for the inclusion of M as an intermediate metabolite and simplifying assumptions for A and B.

population model for the cellular kinetics of 3TC in the peripheral blood mononuclear cells (PBMCs) of HIV-1-infected adolescents that incorporates information from laboratory studies and data from clinical studies of infected patients. A two-part approach is employed to link the ex vivo and clinical studies. In the ex vivo analysis, population modeling is used in order to combine the data available from multiple studies of PBMCs from healthy subjects incubated over various time periods and at different concentrations of 3TC. For the analysis of the clinical study data, Bayesian population modeling that uses the ex vivo population model as prior information to develop a population model for 3TC cellular kinetics in infected adolescents is employed.

MATERIALS AND METHODS

Ex vivo experiment design. Peripheral blood mononuclear cells from 12 healthy volunteers were isolated from patient donor rings by separation using Ficoll-Hypaque. Cells were cultured for 1, 2, or 4 h or for 16 or 24 h with 1 or 5 mM 3TC with 0.5 mCi/ml ^{3}H-labeled 3TC (33). After incubation, the cells were separated from the medium by centrifugation through oil and extracted with buffered 70% MeOH. These samples were separated by high-performance liquid chromatography, and the counts were determined by liquid scintillation counting. Amounts of intracellular 3TC, 3TC monophosphate (3TCMP), 3TC diphosphate (3TCDP), 3TC triphosphate (3TCTP), and an unidentified 3TC metabolite (M) were normalized to the cell count.

Clinical study design. Patient samples were obtained from participants in the Pediatric AIDS Clinical Trials Group 1012, a phase I, randomized, crossover study of two schedules of combination NRTI therapy with ZDV and 3TC administered as the commercially available combination product Combivir. HIV-infected adolescents, aged 12 to 24 years, who had received at least 4 weeks of treatment with ZDV and 3TC given individually or as Combivir immediately

prior to study entry and who had CD4$^+$ cell counts greater than 250 cells/mm^3 were eligible for enrollment (32). Patients were randomized to one of two groups: initial therapy with two Combivir tablets (600 mg ZDV, 300 mg 3TC) administered once daily for the initial phase, followed by either one Combivir tablet (300 mg ZDV, 150 mg 3TC) administered twice daily (group A) or by once-daily dosing (group B). Subjects were maintained on their once-daily regimen for 7 days, and pharmacokinetic studies were completed. Intensive pharmacokinetic samples were collected during the once-daily regimen only, and thus, only the subjects from study group B were used in this analysis. The clinical study protocol was approved by institutional review boards, and all patients provided written informed consent. Compliance prior to the pharmacokinetic study was confirmed by a patient diary and tablet counts.

Blood samples from 24 patients were obtained immediately prior to the 3TC and ZDV doses and at 2, 4, 6, 12, and 24 h postdose. For each blood sample, PBMCs were isolated with BD CPT tubes and extracted with buffered methanol. The 3TC metabolites were separated by using Waters QMA (anion-exchange) SPE cartridges and by eluting and collecting the desired metabolite fractions with increasing KCl concentrations. Phosphates were removed by adjusting the pH of the fractions with sodium acetate and cleavage with acid phosphatase. The samples were desalted using Waters C-18 SPE cartridges and then dried and reconstituted, and the resulting 3TC samples were quantitated using a 3TC radioimmunoassay (30). Intracellular 3TC and M concentrations in the patient samples were not determined. Lamivudine in plasma was measured by radioimmunoassay and used to characterize systemic pharmacokinetics.

Phosphorylation pathway model. The schema in Fig. 1A shows the major pathways and intermediates for the transport and metabolism of 3TC. Hydrophilic nucleoside analogs are transported across the cell membrane by functional transporters. Lamivudine is transported into and out of the cell by passive diffusion and human equilibrative nucleoside transporters, which translocate 3TC down its concentration gradient (3). Deoxycytidine kinase catalyzes the phosphorylation and dephosphorylation of 3TC and 3TCMP (6, 7), and CMP/dCMP kinase catalyzes the reaction between 3TCMP and 3TCDP (25). Both 3-phosphoglycerate kinase and nucleoside diphosphate kinases catalyze the reaction between 3TCDP and 3TCTP (21, 22, 23). Finally, catabolism of 3TCTP,

binding to reverse transcriptase, and incorporation into DNA were represented as a single composite pathway.

The unidentified metabolite M is incorporated as a 3TC recycling pathway analogous to the salvage pathway of cytidine. There are alternative cytidine pathways, including pathways for the biosynthesis of phospholipids and the activation of sialic acids (N-acetylneuraminic acid in humans) (18, 19, 37), that sustain a pool of nucleotides, which are plausible pathways for intracellular 3TC metabolism. The biosynthesis of phospholipids involves at least three different pathways, with intermediates that include CDP-choline, CDP-ethanolamine, and CDP-diacylglycerol. The activation of sialic acids involves CMP-sialic acid as the intermediate. Both types of salvage pathways result in the cleavage of CTP to an intermediate metabolite and then to CMP (18, 19, 37). The enzymes that catalyze these pathways for cytidine may catalyze similar reactions for the 3TC metabolites. M is proposed to be an intermediate in the recycling of 3TC, which is necessary for mass balance of parent and intracellular metabolites.

Population modeling. Separate population analyses were performed for the ex vivo data, the systemic 3TC patient data, and the intracellular 3TC metabolite patient data. For ex vivo 3TC phosphorylation analysis, the 1 μM and 5 μM data were combined, and three different candidate models were evaluated based on an exploratory analysis and the known pathways for 3TC metabolism. For the systemic pharmacokinetic analysis of 3TC, consistent with previous studies (15), a two-compartment zero-order absorption model was used in the population analysis (the sampling schedule with its initial observation at 2 h postdose precluded the use of a first-order absorption model). The duration of the absorption was fixed at 1 h for 20 patients and 3 h for 4 patients whose peak concentrations were measured at 4 h postdose. For the population modeling of the intracellular kinetics in the patients, the systemic pharmacokinetic parameters for each patient were used to define the 3TC extracellular concentration-time profile. The model obtained from the ex vivo intracellular data was then used as prior information, together with the predicted systemic concentration profiles, for the population analysis of the intracellular disposition of 3TC in patients during chronic therapy. Because of limitations in the clinical study data, an independent population analysis of the cellular kinetics of 3TC based on the patient data alone was not possible.

All population modeling was performed using WinBUGS, a general-purpose program for Bayesian analysis of complex models using Markov chain Monte Carlo methods (26). For all models, the parameters (θ) were assumed to be jointly lognormally distributed [i.e., $\theta \sim LN(\mu, \Sigma)$] via log transformation. The errors associated with the outputs were assumed to be multiplicative (implemented by log transforming the measured data). The errors of the transformed outputs were taken to be independent and identically distributed for each output with distributions [$N(0, \sigma_k^2)$]. The Bayesian population analysis problem involved estimating μ, Σ^{-1}, σ_k ($k = 1, \ldots, 5$), and individual subject parameters, θ_i ($i = 1, \ldots, 12$), for each model.

In the Bayesian analysis, very broad prior distributions (noninformative prior) were used for the population mean, variance, and error variance parameters for all the ex vivo models considered as well as the systemic pharmacokinetic model. The prior distribution of the population mean parameters (μ) was taken to be independent and normally distributed, each with a large variance of 10^4 and with a mean obtained from a naïve pooled data analysis of the models tested. The prior distribution of the population precision (Σ^{-1}) was assumed to be a Wishart distribution (see reference 26) with an identity matrix as the scale matrix and with the degrees of freedom equal to the number of model parameters. The prior distribution of the standard deviation of the output errors was assumed to be an inverse gamma distribution, with the shape and scale parameters both set to 0.001. The parameter estimates (θ) obtained from the naïve pooled data analysis of each model were used as initial values for the parameters of each individual.

In modeling 3TC metabolism for the HIV-1-infected patients, the population distribution estimated from the final ex vivo model was used as the prior distribution in the Bayesian analysis (informative prior). The rate constants for the transport of 3TC were fixed at their mean values obtained from the final ex vivo model, because intracellular 3TC was not measured in the PBMCs from patients. The prior mean value for μ was set at its value estimated from the ex vivo model. The prior covariance for μ was set as a diagonal matrix, with the diagonal elements equal to the standard errors obtained for the estimated means from the ex vivo model. The prior distribution of the population precision (Σ^{-1}) was assumed to be a Wishart distribution with the mean estimate from the ex vivo model for Σ^{-1} divided by the degrees of freedom (12), as the scale matrix, and the degrees of freedom equal to 12 (number of subjects used for the ex vivo modeling).

Model selection for the ex vivo population modeling analysis was based on the convergence of the WinBUGS estimates of the population parameter means and covariances and the deviance information criterion (DIC) (see reference 26).

TABLE 1. Means and standard deviations of 3TC metabolites at 24 h in the 1 μM and 5 μM experiments and their ratios

3TC metabolite	Mean amt (pmol/10^6 cells) of metabolite ± SD		Ratio (5 μM/1 μM)
	1 μM	5 μM	
3TC (intracellular)	0.33 ± 0.05	1.80 ± 0.29	5.43
3TCMP	0.28 ± 0.08	0.59 ± 0.18	2.08
3TCDP	1.82 ± 0.26	4.00 ± 0.64	2.21
3TCTP	1.61 ± 0.21	3.41 ± 0.61	2.12
M	0.64 ± 0.09	1.32 ± 0.19	2.05

Convergence was assessed by inspection of the Markov chains for the parameters as well as through the use of formal convergence analysis methods associated with WinBUGS.

RESULTS

Exploratory data analysis. Table 1 summarizes the amounts (means ± standard deviations) of each metabolite at 24 h from the experiments using 1 μM and 5 μM extracellular 3TC concentrations along with the ratio of each metabolite for the 5 μM to 1 μM experiments. While the average intracellular 3TC measurement from the 5 μM experiments is 5.4 times its value from the 1 μM experiments, the increase of the metabolites in the 5 μM experiments ranged from 2.05 to 2.21 times the corresponding values from the 1 μM experiments. This suggests that transport kinetics are linear in this concentration range but that the phosphorylation of 3TC is saturable and was therefore modeled as a Michaelis-Menten reaction.

In contrast to previous reports that the phosphorylation of 3TCDP to 3TCTP is the rate-limiting step in the cellular metabolism of lamivudine (27), inspection of the raw data suggested that 3TCDP and 3TCTP are in rapid equilibrium. The ratio of the concentration of 3TCTP to that of 3TCDP was calculated for each individual at each time point, and a linear regression was performed (ratio versus time for all subjects). The slope of the resulting regression line (results not shown) was not significantly different from zero ($P = 0.46$). Thus, 3TCDP and 3TCTP were assumed to be in equilibrium, and their ratio was represented by an unknown partition coefficient ($R_{TP/DP}$) for the candidate models discussed below.

Ex vivo 3TC cellular metabolism model. Based on the phosphorylation pathway model (Fig. 1A) and exploratory data analysis conclusions, population analyses were performed using several candidate models. Following an analysis of the convergence of the candidate models and the values of the DIC model selection criterion, it was concluded that the final model as shown in Fig. 1B was sufficient to describe the data from the ex vivo experiments. In the model, 3TCMP and 3TCDP are in equilibrium (represented by $R_{DP/MP}$), and the amount of 3TCTP catabolized is negligible relative to the amount recycled.

The estimated values for the population mean and intersubject population standard deviation and error variance for the ex vivo experiments are shown in Table 2. The resulting individual subject parameter estimates were used to predict the intracellular time profile for each subject, which are plotted with the corresponding measurements of intracellular 3TC, 3TCMP, 3TCDP, 3TCTP, and M in Fig. 2 (1 μM experiment)

TABLE 2. Population parameter estimates for 3TC metabolism in PBMCs ex vivo

Parameter (unit)	Estimate	
	Population mean	Population SD (CV%)
k_{in} (pmol/10^6 cells/μM/h)	1.35	1.13 (84)
k_{out} (h^{-1})	3.76	3.31 (88)
K_m (pmol/10^6 cells)	0.64	0.36 (56)
V_{max} (pmol/10^6 cells/h)	2.01	0.92 (46)
k_{MP-3TC} (h^{-1})	2.75	1.45 (53)
$R_{DP/MP}$ (−)	8.29	4.37 (53)
$R_{TP/DP}$ (−)	0.91	0.41 (45)
k_{TP-M} (h^{-1})	0.15	0.07 (47)
k_{M-MP} (h^{-1})	0.54	0.36 (67)
σ_{3TC}		0.095 (0.069–0.14)[a]
σ_{3TCMP}		0.098 (0.072–0.14)[a]
σ_{3TCDP}		0.20 (0.15–0.28)[a]
σ_{3TCTP}		0.24 (0.17–0.35)[a]
σ_M		0.12 (0.090–0.17)[a]

[a] Median value (95% credibility interval).

and Fig. 3 (5 μM experiment). The dashed lines in the figures are model predictions using the estimated population mean estimates shown in Table 2. The coefficients of determination (R^2) for the intracellular 3TC, 3TCMP, 3TCDP, 3TCTP, and M for both the 1 μM and 5 μM experiments combined were 0.90, 0.97, 0.99, 0.98, and 0.99, respectively.

Systemic 3TC pharmacokinetics. The population parameters for the 3TC systemic pharmacokinetic model estimated from the 3TC plasma concentration data are shown in Table 3. To evaluate goodness of fit, the model predictions for each subject are plotted against the measured data in Fig. 4, resulting in an R^2 value of 0.88. The estimate for CL/F (47.8 liters/h) in Table 3 is higher than that reported previously by Moore et al. (27) using a one-compartment, first-order absorption model (25.1 liters/h). This may reflect differences in the population as well as the limited number ($n = 6$) of measurements and timing of samples in the current study, which were selected in order to produce informative intracellular data. The systemic 3TC pharmacokinetics predicted for each individual were used as the input function for the subsequent modeling of the intracellular data from the HIV-1-infected patients.

Model for cellular 3TC metabolism in HIV-1-infected patients. The estimated values for the population mean, intersubject standard deviation, and error variance for the intracellular 3TC model are shown in Table 4. Predictions using the population means of the parameters from Table 4 are shown in
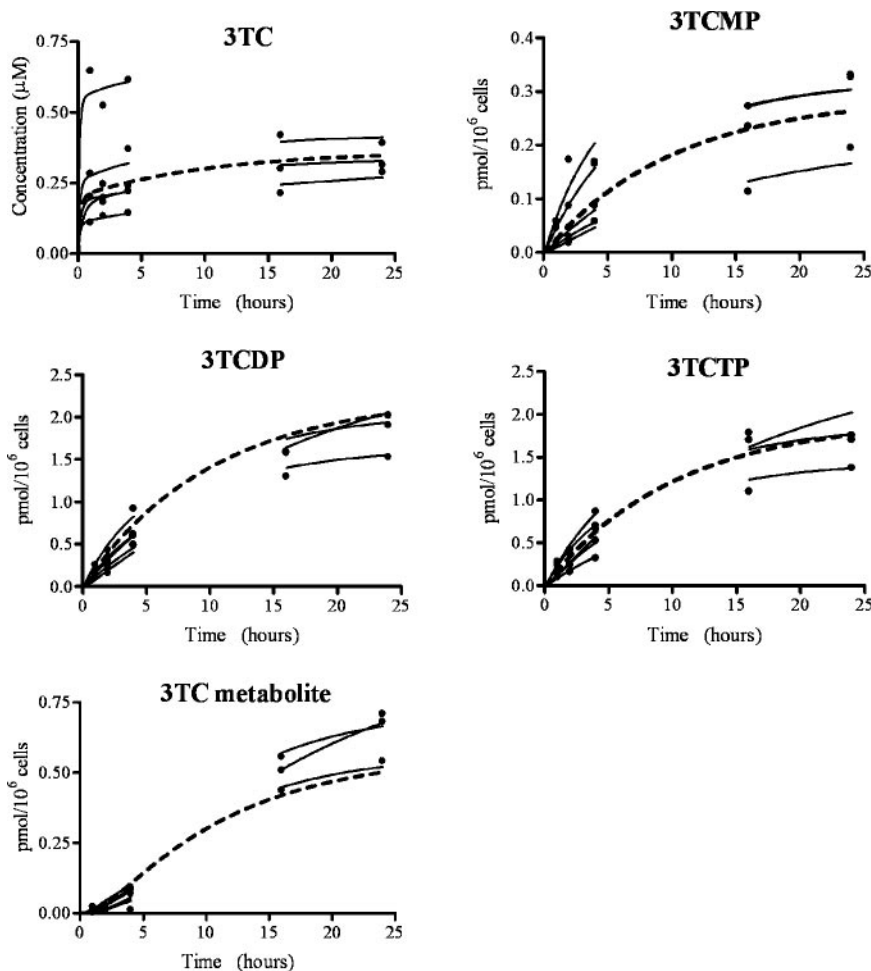

FIG. 2. Ex vivo population (dashed line) and individual (solid line) predictions and measured data (●) (1 μM experiments).
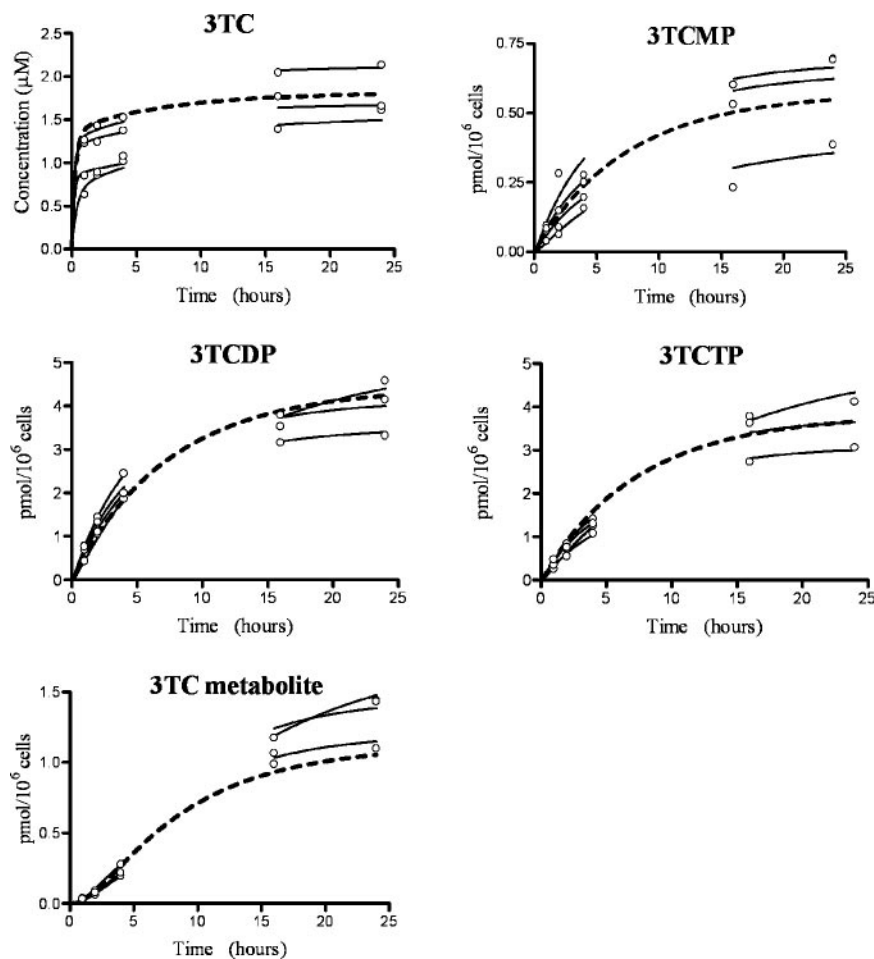
FIG. 3. Ex vivo population (dashed line) and individual (solid line) predictions and measured data (○) (5 μM experiments).

Fig. 5. The variability in the 3TC metabolites is due in part to intersubject variability in both systemic pharmacokinetics and intracellular kinetics. The model predictions for each intracellular 3TC metabolite from all patients are plotted against the measured data in Fig. 6. The R^2 value for each metabolite ranged from 0.33 (for 3TCMP) to 0.75 (for 3TCTP), with an R^2 value of 0.72 for all species combined. The model parameters for intracellular 3TC disposition estimated from patient data (Table 4) are similar to those from the ex vivo experiments (Table 2).

DISCUSSION

In contrast to many therapeutic agents, the activity and toxicity of nucleoside analogs depend on intracellular disposition in addition to systemic pharmacokinetics. Intensive intracellular disposition studies in patients, analogous to those per-

TABLE 3. Population means and standard deviations of 3TC systemic pharmacokinetic parameters

Parameter (unit)	Population mean	Population SD (CV%)
CL/F^b (liters h^{-1})	47.8	21.3 (45)
k_{12} (h^{-1})	0.061	0.047 (77)
k_{21} (h^{-1})	0.060	0.040 (67)
V/F^c (liters)	197	103 (52)
σ_{3TC}		0.40 (0.33–0.49)^a

^{a} Median value (95% credibility interval).
^{b} Apparent clearance.
^{c} Apparent volume of distribution of the central compartment.
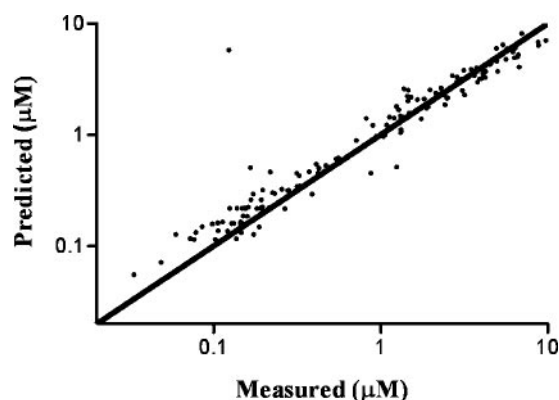

FIG. 4. Predicted versus measured plasma 3TC concentration ($R^2 = 0.88$). The line of unity is also shown.

TABLE 4. Population parameter estimates for 3TC metabolism in
PBMCs from HIV-1-infected adolescents

Parameter (unit)	Estimate	
	Population mean	Population SD (CV%)
K_m (pmol/10⁶ cells)	0.58	0.33 (57)
V_{max} (pmol/10⁶ cells/h)	1.95	0.96 (49)
k_{MP-3TC} (h^{-1})	2.02	0.90 (45)
$R_{DP/MP}$ (−)	6.65	2.98 (45)
$R_{TP/DP}$ (−)	1.02	0.89 (87)
k_{TP-M} (h^{-1})	0.16	0.092 (58)
k_{M-MP} (h^{-1})	0.46	0.20 (43)
σ_{3TCMP}		0.87 (0.74–1.05)[a]
σ_{3TCDP}		0.63 (0.54–0.76)[a]
σ_{3TCTP}		0.64 (0.55–0.77)[a]

[a] Median value (95% credibility interval).

formed to determine systemic pharmacokinetics, are limited by the accessibility and number of measurements that can be obtained. The overall aim of this analysis was to integrate data from 3TC ex vivo studies of intracellular uptake and phosphorylation in relevant human cells (PBMCs) with systemic 3TC pharmacokinetic data and the available intracellular anabolite data in order to develop a comprehensive model for the phosphorylation of 3TC in PBMCs as target cells. Central to this effort was the application of Bayesian population modeling that allowed results from the ex vivo analysis to be used as prior information in the population modeling involving the more limited clinical data. The resulting model provides useful insights into 3TC disposition in HIV-1-infected adolescents and supports the feasibility and utility of the ex vivo/clinical modeling approach for other drugs for which intracellular pharmacology is a major determinant of activity.

The population model developed for 3TC transport and phosphorylation from ex vivo experiments using PBMCs from uninfected individuals was able to predict the measured individual concentrations of intracellular 3TC and its metabolites throughout the time course of 24 h. The model provides a number of important insights regarding intracellular 3TC metabolism (Fig. 1B and Table 2). The phosphorylation of 3TC to 3TCMP is saturable, which results in a less-than-proportional increase of intracellular 3TC metabolites relative to the extracellular concentration. The estimated population mean of K_m is 0.64 pmol/10⁶ cells, which is higher than the mean 24-h intracellular 3TC value from the 1 μM experiments (0.33 ± 0.05 pmol/10⁶ cells) but lower than the corresponding values from the 5 μM experiments (1.80 ± 0.29 pmol/10⁶ cells). The potential saturability of this initial phosphorylation step (K_m = 0.58 pmol/10⁶ cells in the clinical population model) has important implications for adjusting systemic doses to increase antiretroviral activity.

The model without a 3TCTP catabolic pathway was sufficient to describe intracellular 3TC in the ex vivo studies (Fig. 2 and 3) and in patients (Fig. 6). This is consistent with previous studies that reported that 3TCTP is not susceptible to deamination by aminohydrolase or phosphorolysis by human platelet pyrimidine nucleoside phosphorylase, which are the two known pathways of cytidine and deoxycytidine degradation (4). The persistence of 3TCTP and triphosphates of similar nucleosides including zidovudine, didanosine, and abacavir in lymphocytes is substantially longer than systemic concentrations and has provided the basis for dose schedules (1, 12, 34). The modeling results of this study indicate that the persistence of 3TCTP in PBMCs is a function of the overall intracellular pool of 3TC and phosphorylated metabolites rather than a consequence of triphosphate catabolism.
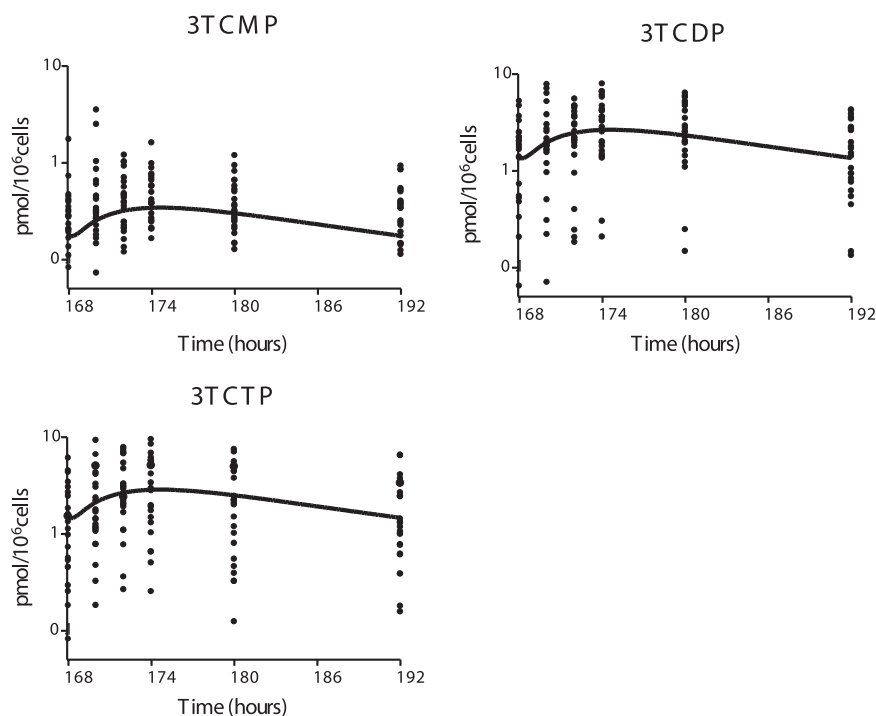

FIG. 5. Prediction (using the population mean values shown in Table 4) of the 3TC metabolite concentrations for the clinical study.
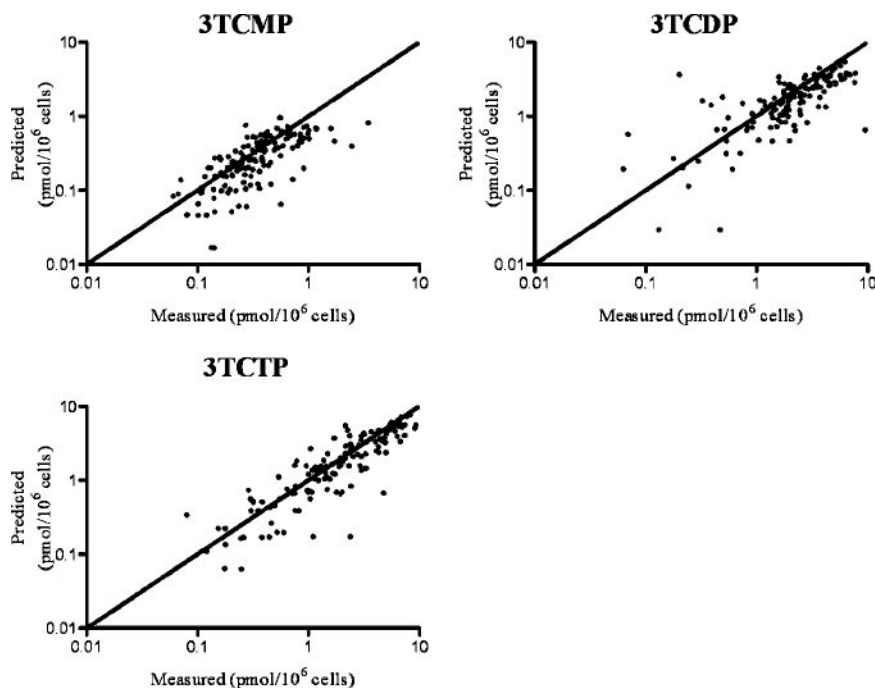
FIG. 6. Clinical population model predictions versus measured data for each patient (R^2 values of 0.33, 0.51, and 0.75 for 3TCMP, 3TCDP, and 3TCTP, respectively). The line of unity is also shown.

There is a relatively rapid equilibrium between 3TCMP and 3TCDP and between 3TCDP and 3TCTP over the course of the measurements. The equilibrium between 3TCDP and 3TCTP is evident from the raw data and is supported by the parameter estimates from the model. While the equilibrium between 3TCMP and 3TCDP is not as obvious from the raw data, the Bayesian population analyses resulted in a smaller DIC value for the model incorporating 3TCMP-3TCDP equilibrium versus the corresponding candidate model with the phosphorylation and dephosphorylation steps modeled as first-order processes.

The model includes a recycling pathway from 3TCTP to 3TCMP via the metabolite M that has been previously detected (35), but the importance of this metabolite to the overall intracellular phosphorylation has not been established. While the metabolite M has not been definitively identified, given the known pathways involving metabolites of the endogenous analogs of 3TC (cytidine and deoxycytidine), it is reasonable that the process of 3TC metabolism in PBMCs involves a recycling pathway. Solas et al. previously measured a metabolite in stimulated PBMCs from uninfected subjects incubated with 3TC and in PBMCs from a single HIV-1-infected patient on the oral regimen of the drug (35). Based on enzyme digestion of the metabolite fraction using alkaline phosphatase plus phosphodiesterase, the metabolite was assumed to be 3TCDP-choline, which is consistent with similar studies with zalcitabine (dideoxycytosine) (20). The modeling results reported here establish this intermediate metabolite as necessary for describing intracellular 3TC metabolism.

The population means and intersubject variabilities for the cellular kinetic model parameters obtained from the HIV-1-infected patients and from the ex vivo study are similar. Several factors, including HIV-1 infection and concomitant administration of ZDV, could alter the cellular disposition of 3TC in PBMCs of the patients relative to that of uninfected subjects studied ex vivo and thus call into question the validity of using the ex vivo model parameters as prior information in the clinical study population analysis. Infection with HIV-1 is associated with elevated concentrations of cellular activation markers compared to those of healthy PBMCs (2), which can lead to significantly increased levels of ZDV phosphorylation in PBMCs (12, 36). For 3TC, however, the relative increase in intracellular 3TCTP in stimulated versus resting PBMCs is smaller than that of ZDV (12). Moreover, the patients in our study were relatively healthy, with a low percentage of their PBMCs in the stimulated state. The concomitant administration of ZDV in patients could also alter 3TC phosphorylation relative to that in the ex vivo studies, since ZDV has been shown to reduce the amount of 3TCTP formed in phytohemagglutinin-stimulated PBMCs via its action on deoxycytidine kinase (20). Since the majority of PBMCs in our patient population are in the resting state, we concluded that it is reasonable to assume that there is no significant inhibition of deoxycytidine kinase by ZDV, at least not to the extent that it would invalidate the use of the ex vivo experiment to serve as prior information for the clinical experiment population modeling analysis. These factors, and other differences between the ex vivo and clinical studies (e.g., exposure profile), did not result in substantive overall differences in the estimated population parameters between the ex vivo and clinical studies presented in this report. It should be noted, however, that a significant portion of the variability in the intracellular data observed in the clinical studies was attributed to within-subject residual variability in the population analysis, which includes protocol

deviations, model misspecification, and analytical errors. Nevertheless, the population model for the cellular kinetics of 3TC in the PBMCs of HIV-1-infected adolescents presented in this report (model structure and parameter distribution) predicts the observed cellular kinetics of 3TCTP with reasonable fidelity.

In a concentration-controlled trial, Anderson et al. previously found higher concentrations of intracellular 3TCTP in female patients than in males (1). Neither sex nor other covariates such as age and race were found to be statistically significant predictors of cellular kinetic model parameters in our study, perhaps due to the small size of our study (24 patients in total). In addition, the concentration-controlled paradigm used previously (1) is a more powerful design for detecting differences in cellular kinetics related to sex or other covariates.

The approach presented here provides a framework for bridging ex vivo and clinical studies of cellular 3TC kinetics that may be used for the study of other NRTIs whose cellular kinetics are a major factor contributing to the persistence of the triphosphate concentrations in CD4 cells in HIV-1-infected patients. Unanticipated clinical outcomes with NRTI therapy including early virological failure (11) and negative effects on immunological reconstitution (17, 28) have not been sufficiently addressed by ex vivo studies alone, as illustrated by studies of the interaction of tenofovir and didanosine (31). The successful application of this modeling strategy to link laboratory and clinical data for 3TC suggests the possibility of extending this approach to examining the determinants of activity and adverse effects of other NRTI-based antiretroviral regimens.

REFERENCES

1. **Anderson, P. L., T. N. Kakuda, S. Kawle, and C. V. Fletcher.** 2003. Antiviral dynamics and sex differences of zidovudine and lamivudine triphosphate concentrations in HIV-infected individuals. AIDS **17:**2159–2168.
2. **Anderson, P. L., T. N. Kakuda, and K. A. Lichtenstein.** 2004. The cellular pharmacology of nucleoside- and nucleotide-analogue reverse-transcriptase inhibitors and its relationship to clinical toxicities. Clin. Infect. Dis. **38:**743–753.
3. **Cabrita, M. A., S. A. Baldwin, J. D. Young, and C. E. Cass.** 2002. Molecular biology and regulation of nucleoside and nucleobase transporter proteins in eukaryotes and prokaryotes. Biochem. Cell Biol. **80:**623–638.
4. **Cammack, N., P. Rouse, C. L. Marr, P. J. Reid, R. E. Boehme, J. A. Coates, C. R. Penn, and J. M. Cameron.** 1992. Cellular metabolism of (−) enantiomeric 2′-deoxy-3′-thiacytidine. Biochem. Pharmacol. **43:**2059–2064.
5. **Carr, A.** 2003. Toxicity of antiretroviral therapy and implications for drug development. Nat. Rev. Drug Discov. **2:**624–634.
6. **Chang, C. N., S. L. Doong, J. H. Zhou, J. W. Beach, L. S. Jeong, C. K. Chu, C. H. Tsai, Y. C. Cheng, D. Liotta, and R. Schinazi.** 1992. Deoxycytidine deaminase-resistant stereoisomer is the active form of (+/−)-2′3′-dideoxy-3′-thiacytidine, in the inhibition of hepatitis B virus replication. J. Biol. Chem. **267:**13938–13942.
7. **Chang, C. N., V. Skalski, J. H. Zhou, and Y. C. Cheng.** 1992. Biochemical pharmacology of (+)- and (−)-2′,3′-dideoxy-3′-thiacytidine as anti-hepatitis B virus agent. J. Biol. Chem. **267:**22414–22420.
8. **Fletcher, C. V.** 1999. Pharmacologic considerations for therapeutic success with antiretroviral agents. Infect. Dis. **33:**989–995.
9. **Fletcher, C. V., P. L. Anderson, T. N. Kakuda, T. W. Schacker, K. Henry, C. R. Gross, and R. C. Brundage.** 2002. Concentration-controlled compared with conventional antiretroviral therapy for HIV infection. AIDS **16:**551–560.
10. **Furman, P. A., J. A. Fyfe, M. H. St. Clair, K. Weinhold, J. L. Rideout, G. A. Freeman, S. N. Lehrman, D. P. Bolognesi, S. Broder, H. Mitsuya, and D. W. Barry.** 1986. Phosphorylation of 3′-azido-3′-deoxythymidine and selective interaction of the 5′-triphosphate with human immunodeficiency virus reverse transcriptase. Proc. Natl. Acad. Sci. USA **83:**8333–8337.
11. **Gallant, J. E., A. E. Rodriguez, W. G. Weinberg, B. Young, D. S. Berger, M. L. Lim, Q. Liao, L. Ross, J. Johnson, and M. S. Shaefer.** 2005. Early virologic nonresponse to tenofovir, abacavir, and lamivudine in HIV-infected antiretroviral-naive subjects. J. Infect. Dis. **192:**1921–1930.
12. **Gao, W. Y., R. Agbaria, J. S. Driscoll, and H. Mitsuya.** 1994. Divergent anti-human immunodeficiency virus activity and anabolic phosphorylation of 2′,3′-dideoxynucleoside analogs in resting and activated human cells. J. Biol. Chem. **269:**12633–12638.
13. **Hart, G. J., D. C. Orr, C. R. Penn, H. T. Figueiredo, N. M. Gray, R. E. Boehme, and J. M. Cameron.** 1992. Effects of (−)-2′-deoxy-3′-thiacytidine (3TC) 5′-triphosphate on human immunodeficiency virus reverse transcriptase and mammalian DNA polymerases alpha, beta, and gamma. Antimicrob. Agents Chemother. **36:**1688–1694.
14. **Hogg, R. S., K. V. Heath, B. Yip, K. J. Craib, M. V. O'Shaughnessy, M. T. Schechter, and J. S. Montaner.** 1998. Improved survival among HIV-infected individuals following initiation of antiretroviral therapy. JAMA **279:**450–454.
15. **Johnson, M. A., K. H. Moore, G. J. Yuen, A. Bye, and G. E. Pakes.** 1999. Clinical pharmacokinetics of lamivudine. Clin. Pharmacokinet. **36:**41–66.
16. **Kakuda, T. N.** 2000. Pharmacology of nucleoside and nucleotide reverse transcriptase inhibitor-induced mitochondrial toxicity. Clin. Ther. **22:**685–708.
17. **Kakuda, T. N., P. L. Anderson, and S. L. Becker.** 2004. CD4 cell decline with didanosine and tenofovir and failure of triple nucleoside/nucleotide regimens may be related. AIDS **18:**2442–2444.
18. **Kean, E. L., K. Munster-Kehnel, and R. Gerardy-Schahn.** 2004. CMP-sialic acid synthetase of the nucleus. Biochim. Biophys. Acta **1673:**56–65.
19. **Kennedy, E. P., L. F. Borkenhagen, and S. W. Smith.** 1959. Possible metabolic functions of deoxycytidine diphosphate choline and deoxycytidine diphosphate ethanolamine. J. Biol. Chem. **234:**1998–2000.
20. **Kewn, S., G. J. Veal, P. G. Hoggard, M. G. Barry, and D. J. Back.** 1997. Lamivudine (3TC) phosphorylation and drug interactions in vitro. Biochem. Pharmacol. **54:**589–595.
21. **Kreimeyer A., B. Schneider, R. Sarfati, A. Faraj, J. P. Sommadossi, M. Veron, and D. Deville-Bonne.** 2001. NDP kinase reactivity towards 3TC nucleotides. Antivir. Res. **50:**147–156.
22. **Krishnan, P., J. Y. Liou, and Y. C. Cheng.** 2002. Phosphorylation of pyrimidine L-deoxynucleoside analog diphosphates. J. Biol. Chem. **277:**31593–31600.
23. **Krishnan, P., Q. Fu, W. Lam, J. Y. Liou, G. Dutschman, and Y. C. Cheng.** 2002. Phosphorylation of pyrimidine deoxynucleoside analog diphosphates. J. Biol. Chem. **277:**5453–5459.
24. **Lewis, W., J. F. Simpson, and R. R. Meyer.** 1994. Cardiac mitochondrial DNA polymerase-gamma is inhibited competitively and noncompetitively by phosphorylated zidovudine. Circ. Res. **74:**344–348.
25. **Liou, J. Y., G. E. Dutschman, W. Lam, Z. Jiang, and Y. C. Cheng.** 2002. Characterization of human UMP/CMP kinase and its phosphorylation of D- and L-form deoxycytidine analogue monophosphates. Cancer Res. **62:**1624–1631.
26. **Lunn, D. J., N. Best, A. Thomas, J. Wakefield, and D. Spiegelhalter.** 2002. Bayesian analysis of population PK/PD models: general concepts and software. J. Pharmacokin. Pharmacodyn. **29:**271–307.
27. **Moore, K. H., J. E. Barrett, S. Shaw, G. E. Pakes, R. Churchus, A. Kapoor, J. Lloyd, M. G. Barry, and D. Back.** 1999. The pharmacokinetics of lamivudine phosphorylation in peripheral blood mononuclear cells from patients infected with HIV-1. AIDS **13:**2239–2250.
28. **Negredo, E., J. Moltó, D. Burger, P. Viciana, E. Ribero, R. Paredes, M. Juan, L. Ruiz, J. Puig, A. Pruvost, J. Grassi, E. Masmitja, and B. Clotet.** 2004. Unexpected CD4 cell count decline in patients receiving didanosine and tenofovir-based regimens despite undetectable viral load. AIDS **18:**459–463.
29. **Palella, F. J., Jr., K. M. Delaney, A. C. Moorman, M. O. Loveless, J. Fuhrer, G. A. Satten, D. J. Aschman, and S. D. Holmberg.** 1998. Declining morbidity and mortality among patients with advanced human immunodeficiency virus infection. N. Engl. J. Med. **338:**853–860.
30. **Robbins, B. L., T. T. Tran, F. H. Pinkerton, F. Akeb, R. Guedj, J. Grassi, D. Lancaster, and A. Fridland.** 1998. Development of a new cartridge radioimmu-

noassay for determination of intracellular levels of lamivudine triphosphate in the peripheral blood mononuclear cells of human immunodeficiency virus-infected patients. Antimicrob. Agents Chemother. **42:**2656–2660.

31. **Robbins, B. L., C. K. Wilcox, A. Fridland, and J. H. Rodman.** 2003. Metabolism of tenofovir and didanosine in quiescent or stimulated human peripheral blood mononuclear cells. Pharmacotherapy **23:**695–701.

32. **Rodman, J. H., B. L. Robbins, J. Martinez, J. C. Lindsay, J. F. Rodriguez, and P. M. Flynn.** 2003. Intracellular phosphorylation of zidovudine and lamivudine in PBMCs from HIV-1 infected adolescents on once versus twice daily regimen, p 110. *In* Proceedings of the 10th Conference on Retroviruses and Opportunistic Infections, Boston, Mass.

33. **Rodman, J. H., B. L. Robbins, Z. Zhou, C. L. Wilcox, E. F. Neal, and D. Z. D'Argenio.** 2005. Abstr. 6th Int. Workshop Clin. Pharmacol. HIV Ther., abstr. 47.

34. **Rodman, J. H., B. Robbins, P. M. Flynn, and A. Fridland.** 1996. A systemic and cellular model for zidovudine plasma concentrations and intracellular phosphorylation in patients. J. Infect. Dis. **174:**490–499.

35. **Solas, C., Y. F. Li, M. Y. Xie, J. P. Sommadossi, and X. J. Zhou.** 1998. Intracellular nucleotides of (−)-2′,3′-deoxy-3′-thiacytidine in peripheral blood mononuclear cells of a patient infected with human immunodeficiency virus. Antimicrob. Agents Chemother. **42:**2989–2995.

36. **Tornevik, Y., B. Jacobsson, S. Britton, and S. Eriksson.** 1991. Intracellular metabolism of 3′-azidothymidine in isolated human peripheral blood mononuclear cells. AIDS Res. Hum. Retrovir. **7:**751–759.

37. **Vance, D. E.** 1983. Metabolism of glycerolipids, sphingolipids, and prostaglandins, p. 505–544. *In* G. L. Zubay (ed.), Biochemistry. Addison-Wesley Publishing Co. Inc., Reading, Mass.